



Kent Academic Repository

Liang, Mingzhi, Frank, Stefanie, Lünsdorf, Heinrich, Warren, Martin J. and Prentice, Michael B (2017) *Bacterial microcompartment-directed polyphosphate kinase promotes stable polyphosphate accumulation in E. coli*. *Biotechnology Journal*, 12 (3). ISSN 1860-6768.

Downloaded from

<https://kar.kent.ac.uk/60055/> The University of Kent's Academic Repository KAR

The version of record is available from

<https://doi.org/10.1002/biot.201600415>

This document version

Author's Accepted Manuscript

DOI for this version

Licence for this version

UNSPECIFIED

Additional information

Versions of research works

Versions of Record

If this version is the version of record, it is the same as the published version available on the publisher's web site. Cite as the published version.

Author Accepted Manuscripts

If this document is identified as the Author Accepted Manuscript it is the version after peer review but before type setting, copy editing or publisher branding. Cite as Surname, Initial. (Year) 'Title of article'. To be published in *Title of Journal*, Volume and issue numbers [peer-reviewed accepted version]. Available at: DOI or URL (Accessed: date).

Enquiries

If you have questions about this document contact ResearchSupport@kent.ac.uk. Please include the URL of the record in KAR. If you believe that your, or a third party's rights have been compromised through this document please see our [Take Down policy](https://www.kent.ac.uk/guides/kar-the-kent-academic-repository#policies) (available from <https://www.kent.ac.uk/guides/kar-the-kent-academic-repository#policies>).

Research Article**Title: Bacterial microcompartment-directed polyphosphate kinase promotes stable polyphosphate accumulation in *E. coli***

Mingzhi Liang^{1,2}, Stefanie Frank², Heinrich Lünsdorf³, Martin J Warren^{2*},
Michael B Prentice^{1,4,5*}

¹Department of Microbiology, University College Cork, Cork, Ireland

²School of Biosciences, University of Kent, Canterbury, Kent CT2 7NJ, UK

³Central Facility for Microscopy, Helmholtz Center of Infection Research, Braunschweig,
D-38124, Germany

⁴Department of Pathology, University College Cork, Cork, Ireland

⁵APC Microbiome Institute, University College Cork, Cork, Ireland

Correspondence: Professor Michael B Prentice, Department of Microbiology,
University College Cork, Cork, Ireland

Email: m.prentice@ucc.ie

Keywords: Metabolic engineering; Synthetic biology; Bacteria; Biopolymers;
Microreactors.

Abbreviations: BMC, bacterial microcompartment; EBPR, enhanced biological
phosphorus removal ; PPK1, polyphosphate kinase; PPX, exopolyphosphatase.

1 Abstract

2 Processes for the biological removal of phosphate from wastewater rely on the temporary
3 manipulation of bacterial polyphosphate levels by phased environmental stimuli. In *E. coli*
4 polyphosphate levels are controlled via the polyphosphate-synthesizing enzyme
5 polyphosphate kinase (PPK1) and exopolyphosphatases (PPX and GPPA), and are
6 temporarily enhanced by PPK1 overexpression and reduced by PPX overexpression. We
7 hypothesised that partitioning PPK1 from cytoplasmic exopolyphosphatases would
8 increase and stabilise *E. coli* polyphosphate levels. Partitioning was achieved by co-
9 expression of *E. coli* PPK1 fused with a microcompartment-targeting sequence and an
10 artificial operon of *Citrobacter freundii* bacterial microcompartment genes. Encapsulation
11 of targeted PPK1 resulted in persistent phosphate uptake and stably increased cellular
12 polyphosphate levels throughout cell growth and into the stationary phase, while PPK1
13 overexpression alone produced temporary polyphosphate increase and phosphate uptake.
14 Targeted PPK1 increased polyphosphate in microcompartments 8-fold compared with non-
15 targeted PPK1. Co-expression of PPX polyphosphatase with targeted PPK1 had little effect
16 on elevated cellular polyphosphate levels because microcompartments retained
17 polyphosphate. Co-expression of PPX with non-targeted PPK1 reduced cellular
18 polyphosphate levels. Thus, subcellular compartmentalisation of a polymerising enzyme
19 sequesters metabolic products from competing catabolism by preventing catabolic enzyme
20 access. Specific application of this process to polyphosphate is of potential application for
21 biological phosphate removal.

22

23

1 1. Introduction

2 Polyphosphate is a molecule thought to be present in all organisms [1] playing a role in
3 cellular metabolic processes, stress response processes, virus replication and cell structure
4 [2]. Bacterial polyphosphate accumulation underlies the enhanced biological phosphorus
5 removal (EBPR) process, which uses microorganisms to remove inorganic phosphate (Pi)
6 from wastewater [3]. Phosphate recovery processes are required to reduce eutrophication,
7 the overgrowth of cyanobacteria and plants in water polluted by excess phosphorus from
8 human activity [4], and to recycle phosphate because of the unsustainability of current
9 natural resources beyond the next century [5]. In EBPR, cycling of wastewater sludge
10 through aerobic and anaerobic phases of incubation lasting several hours, when continued
11 over a period of weeks selects a bacterial consortium that has a net effect of removing
12 phosphorus from wastewater over the cycle by accumulating it in the sludge.
13 Polyphosphate-accumulating bacteria are key consortium components [6, 7]. Phosphate
14 release from the consortium occurs in the anaerobic phase in parallel with consumption of
15 volatile fatty acids, polyhydroxyalkanoate polymer formation and glycogen utilisation. In
16 the aerobic phase stored polyhydroxyalkanoate is catabolised, glycogen replenished and
17 phosphate taken up to form polyphosphate granules [7]. EBPR is a complex dynamic
18 process - an uncultured bacterium *Candidatus Accumulibacter phosphatis* performs a key
19 role in EBPR polyphosphate accumulation [8], and a functioning EBPR reactor may cease
20 phosphate removal for unknown reasons [3, 9].

21

22 Genetic manipulation of aspects of phosphate binding, uptake and storage by a single
23 model organism such as *E. coli* has been suggested as an alternative or additive approach

1 to biological phosphorus removal [10–13]. One issue with over-expression of a
2 polyphosphate forming enzyme in *E. coli* has been that most of the consequent increase of
3 polyphosphate is temporary, probably because of the existence of competing catabolic
4 enzymes [14, 15] and phosphate release from the cells then occurs as the polyphosphate is
5 broken down.

6

7 In *E. coli* polyphosphate kinase PPK1 (E.C. 2.7.4.1) is the enzyme responsible for
8 assembling inorganic polyphosphate polymers in the bacterial cytoplasm by catalysing the
9 reaction $n\text{ATP} \rightleftharpoons (\text{polyphosphate})_n + n\text{ADP}$ [16, 17]. Although this is a reversible reaction,
10 in *E. coli* this enzyme generally favours synthesis of polyphosphate over breakdown (V_{max}
11 ratio of 4.1) [17] (Fig. 1A). However, the balance between net accumulation and breakdown
12 changes dynamically during culture growth and also in response to external stimuli such
13 as [anaerobiosis](#), in part due to the action of degradative exopolyphosphatases. In this
14 respect *E. coli* contains two such polyphosphatases that release orthophosphate from the
15 termini of long chain polyphosphate: $(\text{polyphosphate})_n \rightarrow (\text{polyphosphate})_{n-1} + \text{P}_i$. The
16 two polyphosphatases are called PPX (E.C. 3.6.1.11, sometimes referred to as PPX1) [18,
17 19], which is encoded in the same operon as PPK1, and its homologue guanosine
18 pentaphosphate phosphohydrolase (GPPA or PPX2) [17, 20]. GPPA (E.C. 3.6.1.40) also
19 hydrolyses guanosine pentaphosphate (pppGpp) to guanosine tetraphosphate (ppGpp) with
20 phosphate release as part of the control of the stringent response. Both PPX and GPPA are
21 competitively inhibited by pppGpp [21]. Consequently, amino acid starvation in *E. coli*
22 leads to the accumulation of large amounts of polyphosphate due to the high levels of
23 pppGpp produced as part of the stringent response [21]. In *E. coli* *ppk1* and *ppx* are adjacent

Commented [MOU1]: Anaerobiosis: Dictionary definition e.g. Merriam-Webster is “life in the absence of air or free oxygen”. Anaerobiosis

1 genes forming an operon and knockout of *ppx* alone has been engineered by combined
2 knockout of *ppk1* and *ppx* with heterologous plasmid expression of *ppk1* [15, 22, 23].
3 Elevation of polyphosphate levels in these cells rapidly declines a few hours after *ppk1*
4 plasmid induction whether *ppx* is active or knocked out [15], showing that PPX is not the
5 sole cause of instability in polyphosphate levels in *E. coli*. We hypothesized that an
6 alternative approach to prevent the access of all other cytoplasmic enzymes, (not just PPX)
7 to polyphosphate formed from recombinant PPK1 would stabilise cellular polyphosphate
8 levels and create a phosphate-retaining phenotype. The mechanism used to achieve this is
9 targeting of PPK1 to a recombinant bacterial microcompartment.

10

11 Bacterial microcompartments (BMCs) are proteinaceous vesicles found in certain bacteria
12 that house specific metabolic pathways encased within a closed polyhedral shell of 100-
13 150 nm diameter. The shells are made of thin protein sheets [24] containing pores less than
14 1 nm in diameter [25] which can be positively or negatively charged. There are two broad
15 groups of BMCs, those associated with the anabolic process of RuBisCO-mediated carbon
16 fixation (carboxysomes) and those associated with catabolic fermentative processes such
17 as 1,2-propanediol utilisation (metabolosomes) [26, 27]. Although BMCs were first seen
18 over fifty years ago in photosynthetic cyanobacteria [28], their presence in the cytoplasm
19 of heterotrophic bacteria was only confirmed in 1998 [29] after they were detected in thin
20 sections of *Salmonella enterica* grown on 1,2-propanediol. In fact, around twenty per cent
21 of bacterial genome sequences contain BMC structural genes [26], in many cases
22 associated with enzymes of unknown function [30].

23

1 A significant proportion of bacteria therefore make a major investment in retaining and
2 expressing large (15+ gene) operons encoding these structures and associated enzymes. It
3 is believed the structures help mediate metabolic efficiency by selective limitation of the
4 shell pores on the passage of substrates [31], by metabolite channelling, or other unknown
5 mechanisms **resulting in** retention of reaction intermediates within the structure [32, 33].
6 *Salmonella enterica* Serovar Typhimurium accrues a competitive metabolic advantage by
7 BMC-mediated respiration of ethanolamine in a mouse colitis model [34].
8 Enterohaemorrhagic *E. coli* obtains a similar competitive advantage from BMC-mediated
9 ethanolamine fermentation in bovine intestinal fluid [35], favouring persistent intestinal
10 carriage.

11

12 Recombinant BMCs using genes from *Citrobacter freundii* can be expressed
13 heterologously in *E. coli* [36], both with and without [37] the associated interior enzymes.
14 Peptide sequences enabling enzyme localisation to the BMC interior have been identified
15 [37] [38]. For instance, the first 18 amino acids of PduP, P18, or the first 18 or 60 amino
16 acids of PduD (D18 or D60) can be used as fusions to direct “foreign” proteins into the
17 BMC [39]. Compartmentalisation of the cellular interior is a functionally transforming
18 process often thought of as characteristic of eukaryotes [40], but specific localisation of
19 any enzyme to a re-engineered BMC in bacteria could increase metabolic flexibility of the
20 bacterial host enabling novel phenotypes [41]. Nanotechnological applications of
21 biological compartment systems have included the use of viral capsids for DNA delivery
22 [42], lumazine synthase enclosure of HIV protease [43], and the compartmentalisation of
23 a metabolic pathway in a bacterial microcompartment [39]. We hypothesized that directing

1 PPK to a BMC would enhance polyphosphate formation within a cellular compartment and
2 that segregation from the known degradative polyphosphatases and other cytoplasmic
3 enzymes should stabilise accumulation of polyphosphate (Fig.1A).

4

5 **2. Materials and Methods**

6 **Strains, plasmids and culture conditions**

7 *E. coli* was grown in LB or MOPS medium [44] with either 0.5 mM or 1.0 mM K₂HPO₄
8 as indicated. Expression of genes cloned into pET vectors was induced by IPTG in *E. coli*
9 BL21 (DE3) and *E. coli* BL21 Tuner™ (DE3) (Novagen). Strains and plasmids are listed
10 in Table 1 and oligonucleotides in Supplementary Data Table S1. **To reduce background**
11 **expression levels of T7 RNA polymerase causing leaky gene expression prior to specific**
12 **IPTG induction, a T7 lysozyme gene was present in all clones on pLysS or its derivative**
13 **pSF37 (pLysS-*pduABJKNU*) unless specifically indicated.** Cultures for phosphate uptake
14 experiments were incubated at 37 °C **and a sample growth curve is shown in**
15 **Supplementary Data Fig. S3A.** When inducing pDuet vectors the incubation temperature
16 was lowered to 18 °C.

17

18 **Molecular biology techniques**

19 Cloning strains used in this study were *E. coli* JM109 or *E. coli* TOP10 (Invitrogen). *E.*
20 *coli* BL21(DE3) and *E. coli* BL21 Tuner™(DE3) were used for expression following
21 standard transformation techniques [45]. For PCR reactions standard protocols were
22 applied using an MJ Research PTC-200 Thermal Cycler for reaction cycles. Genomic DNA

1 was extracted from *E. coli* JM109 using a Wizard® Genomic DNA Purification Kit
2 (Promega). Plasmid constructs were sequenced commercially (GATC Biotech).

3

4 **Targeting of PPK1 to microcompartments**

5 The cloning strategy used to engineer plasmids for targeting of PPK1 to the
6 microcompartment is summarised in Supplementary Data Fig.S1. The *ppk1* gene coding
7 for polyphosphate kinase (PPK1) was PCR-amplified with a proofreading DNA
8 polymerase (Bioline High Velocity Polymerase, Bioline UK, London), using genomic
9 DNA from *E. coli* JM109 as template, using the forward primer PPK1-F and the reverse
10 primer PPK1-R (Table S1). The PCR product was digested with *SacI* and *HindIII*
11 (Fermentas) followed by ligation into pET23b-*pduP18-gfp* digested with *SacI* and *HindIII*.
12 The gene encoding the GFP was replaced by *ppk* with retention of the *pdu* localization
13 sequence *p18*. The ligation product was transformed into *E. coli* Top 10 electrocompetent
14 cells (Invitrogen) by electroporation. The new vector, named pML001 (pET23b-*pduP18*-
15 *ppk1*), was extracted and the *ppk1* insert was sequenced (GATC-Biotech) to confirm no
16 mutation had occurred. Two constructs, pML001 and pLys*SpduABJKNU* (pSF37),
17 expressing empty *pdu* BMCs [37]), were co-transformed into *E. coli* BL21 (DE3) by heat
18 shock.

19 **Co-expression of targeted and untargeted PPK1 and PPX**

20 The pCOLADuet-1 coexpression vector (Novagen) system encoding two multiple cloning
21 sites (MCS) each preceded by a T7 promoter, *lac* operator, and ribosome binding site was
22 used to express targeted and untargeted *E. coli* PPK1 and PPX (*ppx* amplified from *E. coli*

1 JM109) in combination (pYY005, pYY007, pYY008) and alone (pYY002, pYY010) (see
2 Table 1).

3 **Microcompartment purification**

4 Recombinant BMCs were extracted from *E. coli* by modification of the method of Sinha
5 et al [46]. A single colony of *E. coli* BL21(DE3) containing the plasmid encoding
6 microcompartment proteins (pLysS-*pduABJKNU*) was picked and grown in 200 ml of LB
7 to an OD₆₀₀ of 0.4 followed by protein induction with 0.4 mM IPTG. Cells were harvested
8 at OD₆₀₀ 1.0-1.2 and washed twice with 40 ml of buffer A (50 mM Tris-HCl (pH 8.0), 500
9 mM KCl, 12.5 mM MgCl₂, 1.5% 1,2-PD). Cells (1 g wet weight) were resuspended in a
10 mixture of 10 ml of buffer A and 15 ml of B-PER II bacterial protein extraction reagent
11 supplemented with 5mM mercaptoethanol, Complete Protease Inhibitor Cocktail (Roche)
12 at the manufacturer's recommended working dilution, 25 mg of lysozyme, and 2 mg of
13 DNase I. The suspension was incubated for 30 min on a shaking platform at room
14 temperature and on ice for 5 min. After initial removal of cell debris by centrifugation at
15 12,000 x *g* for 5 min at 4°C (repeated twice), the BMC fraction was pelleted by spinning
16 at 20,000 x *g* for 20 min at 4°C. The pellet was washed once with a mixture of 4 ml of
17 buffer A and 6 ml of B-PER II and resuspended in 0.5 ml of buffer B (50 mM Tris-HCl pH
18 8.0, 50 mM KCl, 5 mM MgCl₂, 1% 1,2-PD) containing protease inhibitor. Remaining cell
19 debris was removed by centrifugation for 1 min at 12,000 x *g* at 4°C (repeated three times).
20 Aliquots (50 µg) of extracted protein were separated by SDS-PAGE using a 15%
21 polyacrylamide gel under denaturing conditions in a MiniProtean apparatus (Bio-Rad) and
22 stained with Coomassie Brilliant Blue R250 (Fig.1B). To confirm the identity of proteins
23 peptide fingerprinting by MALDI-TOF-MS (matrix assisted laser desorption/ionization-

1 **time of flight mass spectroscopy**) was carried out as previously described [47].
2 Microcompartments used in ATP regeneration assays (Fig. 1C,D) and whole cell
3 polyphosphate assays (Fig 2) were initially extracted with CelLytic B (Sigma-Aldrich)
4 instead of B-PER II because of reported efficacy of this reagent for polyphosphate
5 extraction [48]. Later comparisons of B-PER II extractions and CelLytic B extractions had
6 shown little difference in measured polyphosphate levels and B-PER II was used for
7 microcompartment extractions shown in Fig. 3. Micrococcal nuclease 2 mg (Sigma-
8 Aldrich) prepared with calcium buffer was substituted for DNase 1 for all
9 microcompartment extractions where polyphosphate was assayed because of the potential
10 adverse effect of Mg²⁺ containing buffers on polyphosphate [49].

11 **ATP regeneration assay to detect PPK1 enzyme activity in microcompartments**

12 A combination of two previously described PPK1 assay methods [48, 50] using luciferase
13 to detect ATP produced from polyphosphate by PPK1 was used as a biochemical screen
14 for the presence of PPK1 and polyphosphate in microcompartment fractions. Briefly, to
15 assay relative PPK1 content 20 µL of BMC extract was added to a 100 µL reaction mixture
16 containing: ultrapure ADP (ATP-free, Cell Technology Inc, Ca), 30 mM MgCl₂, 1% (w/v)
17 Polyphosphate (Sigma), 50 mM Tris-HCl (pH 7.8). The reaction mixture was diluted 1:100
18 in 100 mM Tris-HCl pH 8.0, 4 mM EDTA, of which 0.1 mL was added to 0.1 mL of
19 luciferase reaction mixture from ATP Bioluminescence Assay Kit CLS II (Roche).
20 Luminescence was measured by using a luminometer (Luminoskan, Thermo Labsystems).
21 A standard curve for ATP by dilution in 100 mM Tris-HCl pH 8.0 containing 4 mM EDTA
22 was used to determine PPK1 activity of the extracts (Fig. 1C). To assay relative

1 polyphosphate content, the same reaction omitting added polyphosphate was performed
2 (Figure 1D).

3 **Determination of polyphosphate content of whole cells and extracted** 4 **microcompartments**

5 Polyphosphate concentrations in whole cells presented in Fig. 2A were determined
6 following lysis of pelleted cells from 10 ml of cultures. A metachromatic assay was
7 employed using the 530/630nm absorbance ratio of 10 μ L of lysate added to 1 mL of
8 toluidine dye solution (6 mg/L toluidine blue in 40 mM acetic acid) as described [51]. In
9 later experiments (Fig. 3) polyphosphate was determined by a higher-yielding method
10 using 4'-6-diamidino-2-phenylindole (DAPI) as described previously [52]. For this method
11 cells were harvested by centrifuging at 5000 x g for 10 min at 4° C. After washing in 50
12 mM HEPES buffer (pH 7.5) the cell pellet or purified microcompartment sample was
13 frozen at -20° C followed by defrosting at room temperature. Cell pellets/purified
14 microcompartments were resuspended in HEPES buffer at an appropriate dilution to ensure
15 that the cellular polyP concentration was in the linear range of the DAPI assay (0-6 g
16 polyP/ml). Total assay volume was 300 μ l which included 100 μ L of polyP containing
17 samples and 200 μ L of DAPI assay buffer containing 150 mM KCl, 20 mM HEPES-KOH
18 (pH 7.0) and 10 μ M DAPI solution. After a 10 min incubation at room temperature DAPI
19 fluorescence was measured with a plate reader equipped with excitation and emission
20 filters of 420 nm and 550 nm respectively. **This method was also used to assess the efficacy**
21 **of heat treatment in releasing polyphosphate from cells (Supplementary Data Fig. S4).**

22

1 A polyphosphate standard curve was prepared using sodium phosphate glass Type 45
2 (S4379 Aldrich) and sodium hexametaphosphate (SX0583). Protein concentration of cell
3 extracts was measured using a 10 μ L sample by Bradford assay [53], with Coomassie Plus
4 Protein Assay Reagent (Pierce) with bovine serum albumin as the standard resuspended in
5 the same buffer as the sample.

6

7 **Phosphate uptake** by bacteria from defined media was determined as follows (Fig. 2B).

8 Strains were cultured in LB to OD₆₀₀ 0.4-0.6 and then induced for 1 hr with 0.5 mM of
9 IPTG before being transferred to MOPS medium pH 5.5 [44] containing 0.01 mM iron and
10 0.5 mM potassium phosphate, at an OD₆₀₀ of 0.2. Incubation at 37°C was continued up to
11 48 hrs with intermittent sampling of 0.2 mL. Samples were pelleted by centrifugation and
12 the MOPS medium was analysed for orthophosphate concentration. The cell pellet was
13 analysed for polyphosphate content and protein concentration as described above.
14 Orthophosphate was assayed using a molybdovanadate colorimetric method [54]. 0.2 mL
15 of molybdovanadate solution (Reagecon, cat no: 1056700) was added to 5 mL of culture
16 medium, mixed and incubated at room temperature for 5 min. Optical density of 1 mL was
17 measured at 430 nm against a blank of 4% molybdovanadate in distilled water and a
18 calibration curve of potassium phosphate in MOPS.

19

20 **Light Microscopy**

21 Polyphosphate granules were visualised (Fig. 4) by Neisser's stain using Chrysoidin
22 counterstain [55].

23

1 **Electron microscopy for parallel electron energy loss spectroscopy (PEELS) and**
2 **element mapping by electron spectroscopic imaging (ESI)**

3 Unstained cells were fixed in 3% (v/v) glutaraldehyde, 10 mM Hepes, pH 7.3 (Sigma),
4 dehydrated in an acetone-series and embedded in epoxy resin (Spurr, hard mixture; [56]),
5 as described [57]. For elemental analysis 30 - 40 nm ultrathin sections (otherwise 90 nm
6 for general ultrastructure) were sectioned with a Reichelt-Jung ultramicrotome (Leica,
7 Vienna, Austria), equipped with a diamond knife and were picked up with 300 mesh Cu-
8 grids. Electron micrographs were recorded in the elastic brightfield mode (slit width: 10
9 eV) with an EF-TEM (operated in general at 120 kV acceleration voltage), equipped with
10 an in-column Omega-type energy filter (LIBRA120 plus, Zeiss, Oberkochen Germany), in
11 a magnification range from x 4000 to x 32000 with a bottom-mount cooled 2048 x 2048
12 CCD camera (SharpEye; Tröndle, Moorenweis, Germany).

13

14 **Parallel electron energy loss spectroscopy (PEELS)**

15 Spot-PEELS were recorded within electron dense cytoplasmic inclusion bodies. Spot-size
16 was set to 16 nm and the objective aperture was 60 μm (spectrum magnification: x100;
17 energy range: 67 – 290 eV; recording time: 10 s ; emission current: 1 μA) and the spectrum
18 energy resolution was about 1.6 eV at zero-loss (FWHM). Recorded PEELS data were
19 corrected for background, applying the ‘potence’ underground function of the EsiVision
20 Pro Software (EsiVision Pro, Vers. 3.2; SIS – Soft Imaging Systems, Munster, Germany)
21 and were ‘medium’-filtered (settings: 1.5 eV width).

22

23 **Element mapping by electron spectroscopic imaging (ESI)**

1 Phosphorus mapping was performed as previously described [57] with unstained 35 nm
2 ultrathin sections. According to the '3-window method' energy-windows were set to a
3 dedicated energy loss for the P-L23 edge, as it was given by the corresponding first
4 intensity maximum from the spot-PEELS, i.e. 138 eV (W1: 125 eV; W2: 115 eV). The
5 energy selective slit was set to 6 eV width, and images were recorded with an illumination
6 aperture of 0.63 mrad, an emission current of 1 μ A, a 60 μ m objective aperture, and a
7 nominal magnification of x 6300. Background subtraction for calculating the phosphorus
8 element map was performed by the 'multiwindow exponential difference' method.

9

10 **3. Results**

11 **PPK1 is targeted to recombinant BMCs**

12 The localisation of PPK1 to a recombinant BMC was achieved by engineering a fusion
13 between the known targeting peptide P18 and the N-terminus of PPK1, resulting in P18-
14 PPK1. Recombinant BMCs with the associated P18-PPK1 were isolated from a strain co-
15 producing the *C. freundii* Pdu shell proteins PduABJKNU (pSF37) and P18-PPK1
16 (pML001). Analysis of the purified BMC fraction by SDS-PAGE revealed the presence of
17 P18-PPK1 together with the BMC-associated shell proteins (Fig. 1B).

18

19 A functional assay designed to maximise PPK1's ATP breakdown function was employed
20 to determine the activity of PPK1 when it was directed to the BMC. In comparison to
21 BMCs isolated from cells producing only empty BMCs, or empty BMCs and non-targeted
22 PPK, the purified BMCs from the strain co-producing BMCs and P18-PPK1 generated
23 over twenty-fold more ATP per mg of protein from added polyphosphate (Fig.1C). There

1 was little activity in the equivalent protein fraction prepared using the same
2 microcompartment purification protocol from cells producing only P18-PPK1 in the
3 absence of BMCs. This showed that polyphosphate kinase activity had been transferred to
4 the microcompartments by enzyme targeting.

5

6 The same ATP regeneration assay was repeated in the absence of any added exogenous
7 polyphosphate (Fig.1D). Any ATP generated in this assay would therefore reflect the
8 amount of endogenous polyphosphate within the fraction. The BMC fraction from the cells
9 that co-produced both the BMCs and P18-PPK1 generated more than twice as much ATP
10 as control BMC fractions from cells expressing empty BMCs or BMCs with non-targeted
11 PPK1 (Fig. 1D). This result indicates that the BMCs from strains co-expressing targeted
12 PPK1 had increased levels of polyphosphate, compatible with localisation of PPK1 to the
13 microcompartment and formation of polyphosphate in situ.

14

15 **Effect of PPK1 targeting effect on polyphosphate content and phosphate uptake,**

16 Targeted PPK1 with co-expressed BMCs conferred a distinct cellular phenotype. DAPI
17 negative staining of polyphosphate extracted from whole cells cultured at 37 °C, size-
18 separated on a PAGE gel (Supplementary Data Figure S2), showed that the polyphosphate
19 detected in strains over-expressing either P18-PPK1 alone or P18-PPK1 and BMCs
20 exceeded the length of the sodium phosphate glass Type 45 polyphosphate control. This
21 indicates that long chain polyphosphate is present in these strains. No qualitative difference
22 in chain length was detected between these two clones but long chain polyphosphate in the
23 *E. coli* strain over expressing P18-PPK1 and recombinant BMCs was less evident at time

1 zero but persisted to a later phase of growth (Fig. S2) than in cells expressing P18-PPK1
2 alone. The cells expressing P18-PPK1 alone contained long chain polyphosphate before
3 IPTG induction, probably because of promoter leakage (Supplementary Data Figure S2).
4 No long chain polyphosphate was detected in the *E. coli* control.

5

6 A simultaneous quantitative assay of the cellular polyphosphate and phosphate content of
7 the culture supernatant from the cultures used in the polyphosphate chain length assay was
8 also undertaken. Here, increased phosphate uptake from culture medium was observed in
9 comparison to the host *E. coli* control (Fig. 2B) by both the P18-PPK1-expressing strain
10 and the strain expressing both P18-PPK1 and BMCs. A maximal uptake of approximately
11 0.25 mM at 20 hours was observed for both strains. However, the P18-PPK1-expressing
12 strain returned a third of this phosphate to the supernatant after 48 hours, while the strain
13 expressing both P18-PPK1 and BMCs returned less than 9% of phosphate taken up by 48
14 hours. Correspondingly, the cell-associated polyphosphate levels of the P18-PPK1 strain
15 were maximal at 20 hours and declined thereafter (Fig. 2A), while the P18-PPK1 and
16 BMC-expressing strain retained approximately the same level of cell associated
17 polyphosphate at 48 hours as at 20 hours. The polyphosphate time course was repeated
18 with a simultaneous growth curve and both co-expression of targeted PPK1 and
19 recombinant microcompartments in *E. coli* expression of targeted PPK1 alone caused a
20 similar mild growth retardation to (Supplementary Data Fig. S3).

21

22 **BMCs protect endogenous polyphosphate from exogenous polyphosphatases**

1 Simultaneous expression of polyphosphate-forming PPK1 and the exopolyphosphatase
2 PPX from the pDuet vector in BMC-expressing *E.coli* strains was used to examine the
3 effect of BMC-targeting of these enzymes on cellular polyphosphate accumulation. The
4 induction of non-targeted PPK1 from the pDuet vector increased whole cell polyphosphate
5 levels 5-fold in comparison to control cells containing the BMC shell protein operon and
6 the pDuet vector with no enzyme insert (the enzyme-free control, Fig. 3). It did not increase
7 the polyphosphate content of co-expressed recombinant microcompartments when
8 compared to the enzyme-free control. However, P18-PPK1, when co-produced with the
9 BMCs, increased polyphosphate levels in the BMC fraction 8-fold in comparison to the
10 enzyme-free control, while giving a similar overall 5-fold increase in whole cell
11 polyphosphate to that seen with expression of non-targeted PPK1.

12

13 Co-expression of non-targeted polyphosphatase PPX with non-targeted PPK1 reduced
14 whole cell polyphosphate levels by 50% compared with non-targeted PPK1 expression
15 alone, with little effect on polyphosphate levels in the microcompartment fraction. Co-
16 expression of non-targeted PPX and BMC-targeted P18-PPK1 reduced whole cell
17 polyphosphate levels by 22% and BMC-associated polyphosphate by 18% when compared
18 with microcompartment targeted PPK1 alone. BMC-associated polyphosphate was still at
19 least 2.5 times greater than in cells co-expressing non-targeted PPK1 in the presence or
20 absence of non-targeted PPX. Co-expression of BMC targeted P18-PPK1 with PPX
21 targeted to the microcompartment using a different tag (D60) reduced the BMC-associated
22 polyphosphate content by 50% in comparison to the BMC-targeted P18-PPK1 alone, while
23 reducing whole cell polyphosphate by 22%. The D60 tag was used empirically, to avoid

1 **risking potential interference with targeting caused by using the same tag for two enzymes,**
2 **subsequent experiments outside the scope of this manuscript showed differential tagging**
3 **was unnecessary.** These data suggest that the BMC-targeting of PPK1 results in the
4 synthesis of polyphosphate that is located primarily within the BMC fraction of the cell
5 and is relatively inaccessible to cytoplasmic co-expressed PPX, but more accessible to
6 BMC-targeted PPX. **However, this polyphosphate is released from cells by heat treatment**
7 **(Supplementary Data Figure S4).**

8

9 **Microscopy**

10 Blue-black granules were apparent with Neisser's stain in a proportion of all cells
11 overexpressing P18-PPK1, but not the *E. coli* BL21 (DE3) insert-free control or without
12 any targeted enzyme (Fig. 4). These appearances are consistent with the accumulation of
13 intracellular polyphosphate in *E. coli* cells with increased PPK1 activity. All cells
14 overexpressing P18-PPK1 showed a heterogeneous granule phenotype, with a proportion
15 of non-toluidine blue staining cells in all fields.

16

17 *E. coli* expressing the recombinant microcompartment and P18-PPK1 retained the
18 polyphosphate staining at 44 hours whereas cells expressing P18-PPK1 without the
19 recombinant microcompartment showed reduced staining after 40 hours (Fig. 4).

20 All *E. coli* expressing the recombinant microcompartment had a proportion of cells which
21 were greatly elongated. All *E. coli* forming multiple polyphosphate granules tended to be
22 larger than the non-granulated cells, presumably because of distension by the granules.

1 However, the largest cells were seen with **co-expression** of recombinant
2 microcompartments and **the tagged P18-PPK1 enzyme**.

3

4 **Electron-loss spectroscopic analysis by Energy-filtered Transmission Electron** 5 **Microscopy (EFTEM).**

6

7 Increased phosphorus deposition was detected in all cells expressing recombinant *E.coli*
8 PPK1 by EFTEM (Fig. 5C,D,E,F), verified from PEELS measurement (see below),
9 compared with control *E. coli* strains with no recombinant gene expression (Fig. 5A) or
10 expressing microcompartment genes (Fig. 5B). In cells expressing PPK1 alone, most
11 phosphate signal was represented by particles <5 nm, but some large homogeneous masses
12 > 200 nm with plane edges were visible (Fig. 5C) in a few cells. In cells expressing targeted
13 PPK1 and a recombinant microcompartment operon, in addition to signals from particles
14 <5 nm, multiple phosphate signals from particles 50-100 nm were present (Fig.5D,E,F)
15 and in some cases large circular masses/crescents > 300 nm were present (Fig. 5D,F). These
16 large masses were not homogeneous and appeared composed of small particles and the
17 cells containing them were enlarged. These images appeared similar to light microscopy
18 observations (Fig. 4D,H,L).

19

20 **Parallel electron energy loss spectroscopy (PEELS)**

21 Spot-PEELS recorded from dark inclusions apparent as electron dense regions about 100
22 nm in diameter (Fig 5G), confirmed they contained phosphate, verified from the
23 characteristic ELNES-fingerprint (Energy-Loss Near-Edge Structure) of reference spectra

1 that were recorded from sodium polyphosphate (Fig.5G). The largest polyphosphate
2 inclusion in figure 5E, shown in yellow, is magnified in the inset of the spot-PEELS (Fig.
3 5G); here the 16 nm beam spot and its position are indicated (white circle).

1 4. Discussion

2 Polyphosphate accumulation is the basis of the enhanced biological phosphorus removal
3 (EBPR) process, which uses microorganisms to remove inorganic phosphate (Pi) from
4 wastewater. Accumulation occurs in aerobic conditions as intracellular polyphosphate [8,
5 12] is released as Pi in anaerobic conditions [58] or when the consortium is supplied with
6 organic carbon or heated [12]. The best characterized enzyme responsible for
7 polyphosphate synthesis (PPK1), originally found in *E. coli* [59], can only be detected in
8 silico in the genome sequences of a minority of bacterial genera [60]. The enzyme
9 responsible for polyphosphate synthesis in most bacteria therefore remains to be identified
10 [60].

11

12 In *E. coli*, polyphosphate accumulation in wild-type strains occurs with amino acid
13 starvation or in the stationary phase [21, 50, 61]. Large amounts of polyphosphate
14 accumulate only if the copy number of *ppk1* is increased [14], or a heterologous *ppk* gene
15 is supplied [62], or the phosphate regulatory gene *phoU* is mutated [63, 64]. Even in *E. coli*
16 strains overexpressing *ppk1*, initial accumulation of polyphosphate is known to be partially
17 or completely reversed as the cells reach stationary phase [14, 15]. Because this also occurs
18 in *E. coli* overexpressing *ppk1* with no chromosomal functioning *ppx* gene it has been
19 suggested to be due to either product-induced reversal of the PPK-catalysed reaction, or
20 the activity of another phosphatase enzyme present in the cytoplasm [15]. We observed a
21 similar reversal of polyphosphate accumulation in our overexpressing *ppk1* clone,
22 accompanied by increasing Pi in the culture supernatant (Fig. 2). This did not occur when

1 the *ppk1* gene was engineered to encode an N-terminal BMC localisation sequence (*p18-*
2 *ppk1*) and was expressed in trans with an operon encoding an empty BMC.

3

4 Cells co-producing P18-PPK1 and the empty BMC had a different phosphorus distribution
5 by EFTEM (Fig 5D,E,F) to those expressing PPK1 alone (Fig. 5C), containing single or
6 agglomerated particles in the BMC size range. BMC extractions show the presence of
7 metabolically active PPK1 (Fig.1C,D) and polyphosphate in the BMC fraction
8 (Fig.1D, Fig.3) when PPK1 is microcompartment-targeted in this way. Our results suggest
9 that targeting of PPK1 to a bacterial microcompartment still allows access of the small
10 molecule substrate ATP to the enzyme (Figure 1A), but effectively stabilises the large
11 polymer polyphosphate product (Fig. 2B).

12

13 We hypothesized that this stabilisation results from reduced access of PPX, GPPA or
14 other cytoplasmic phosphatases to the polyphosphate produced by BMC-targeted PPK1.

15 To confirm this we carried out co-expression experiments of PPK1 with PPX (Fig. 3).

16 Co-production of PPX with PPK1 resulted in lower cellular polyphosphate levels than
17 expression of *ppk1* alone (Fig. 3), as has been previously reported [65]. This reduction in
18 total cellular polyphosphate was partially prevented by BMC-association of PPK1, due to
19 increased levels of polyphosphate in the BMC fraction. BMC-targeting of PPK1 therefore
20 results in the synthesis of polyphosphate that is located primarily in the BMC fraction of
21 the cell. Polyphosphate in the BMC fraction is inaccessible to cytoplasmic co-expressed
22 PPX. Adding BMC targeting to PPX using an alternative tag (D60-PPX) co-expressed
23 with targeted PPK1 (P18-PPK1) partially reverses the increase in polyphosphate levels in

1 the BMC fraction conferred by targeted PPK1, presumably by increasing access of the
2 PPX to polyphosphate in the BMC fraction. This suggests that the mechanism of
3 stabilisation of polyphosphate conferred by BMC targeting of PPK1 involves reduced
4 access by cytoplasmic phosphatases.

5

6 Other examples of such macromolecular association of enzymes exist. A variant of
7 lumazine synthase was recently employed to encapsidate HIV protease within an *E. coli*
8 host [43] facilitating recombinant synthesis of this potentially toxic enzyme by separating
9 it from the remaining cytoplasm. Lumazine synthase compartments are genetically
10 unrelated to BMCs involved in catabolic metabolism, and form pentameric components
11 form smaller 30-40 nm icosahedral structures that more closely resemble viral capsids [66].
12 The enzyme is bound to part of the shell molecule forming the inner surface by an
13 electrostatic mechanism [43, 67], (N-terminal fusion displays it on the outside [68]).
14 Enzymically active inclusion bodies can be formed within bacterial cells by C-terminal
15 attachment of short self-assembling peptide sequences [69], or N-terminal fusion with a
16 self aggregating protein [70] but these enzymes are not enclosed within a structure
17 accessed via pores. Subcellular localisation of enzymes catalysing successive reactions in
18 a metabolic pathway to peroxisomes in fungi [71] or BMCs [39] can promote product
19 formation.

20

21 Our results demonstrate that P18-PPK1 is targeted to a recombinant BMC. The
22 observation that polyphosphate accumulates within the BMC suggests that targeted PPK1
23 is internalised within the structure and remains functional, generating polymeric product.

1 ATP must be able to enter the recombinant BMC to allow it to act as one of the substrates
2 for the P18-PPK1 enzyme (Fig. 1A). However, this is not surprising as the native Pdu
3 BMC must allow ATP access as it is required by PduO (located within the
4 microcompartment) for the regeneration of the coenzyme form of cobalamin needed by
5 the diol dehydratase complex [72]. The association of PPK1 with the BMC however
6 leads to sequestration of the enzyme's metabolic product, presumably because its size
7 does not allow it to leave the BMC by the same route by which the enzyme substrate
8 ATP arrived. Protection of the polyphosphate product from catabolism from cytosolic
9 enzymes is therefore achieved, illustrating a general mechanism by which BMC can be
10 used to re-engineer cellular metabolism. The specific polymer generated, polyphosphate,
11 is an important intermediary in the enhanced biological phosphate removal (EBPR)
12 process employing environmental bacteria to remove phosphate from wastewater [3, 12]
13 and has industrial applications [73]. We have shown heat treatment releases
14 microcompartment-located polyphosphate from bacteria (Data Supplement FigS4) as it
15 does from standard EBPR sludge bacteria [74], so recovery of sequestered
16 polyphosphate is readily achievable. EBPR requires prolonged cycles of aerobic and
17 aerobic incubation to operate. The ability to stabilise polyphosphate produced in a single
18 growth phase so that phosphate is not returned to the cell exterior could lead to a
19 streamlined process with a single phase of incubation. This would require transfer of the
20 recombinant microcompartment and targeted polyphosphate kinase from *E. coli* to a more
21 environmentally robust organism, but horizontal transfer of both these components is
22 straightforward. Further evaluation of the properties of any recombinant organism of this

1 type in a closed system would be required before any assessment of the safety of
2 environmental release.

3

4 5. References

- 5 [1] Kulaev, I., Kulakovskaya, T., Polyphosphate and phosphate pump. Annual Review
6 of Microbiology. 2000, 54, 709-734.
- 7 [2] Brown, M.R.W., Kornberg, A., The long and short of it - polyphosphate, PPK and
8 bacterial survival. Trends in Biochemical Sciences. 2008, 33, 284-290.
- 9 [3] Gebremariam, S.Y., Beutell, M.W., Christian, D., Research Advances and
10 Challenges in the Microbiology of Enhanced Biological Phosphorus Removal-A
11 Critical Review. Water Environment Research. 2011, 83, 195-219.
- 12 [4] Smith, V.H., Schindler, D.W., Eutrophication science: where do we go from here.
13 Trends in Ecology & Evolution. 2009, 24, 201-207.
- 14 [5] Sverdrup, H.U., Ragnarsdottir, K.V., Challenging the planetary boundaries II:
15 Assessing the sustainable global population and phosphate supply, using a systems
16 dynamics assessment model. Applied Geochemistry. 2011, 26, S307-S310.
- 17 [6] Fuhs, G.W., Chen, M., Microbiological basis of phosphate removal in the activated
18 sludge process for the treatment of wastewater. Microbial Ecology. 1975, 2, 119-
19 138.
- 20 [7] McMahon, K.D., Read, E.K., Microbial contributions to phosphorus cycling in
21 eutrophic lakes and wastewater. Annual review of microbiology. 2013, 67, 199-219.
- 22 [8] Garcia Martin, H., Ivanova, N., Kunin, V., Warnecke, F., Barry, K.W., McHardy,
23 A.C., Yeates, C., He, S., Salamov, A.A., Szeto, E., Dalin, E., Putnam, N.H.,
24 Shapiro, H.J., Pangilinan, J.L., Rigoutsos, I., Kyrpides, N.C., Blackall, L.L.,
25 McMahon, K.D., Hugenholtz, P., Metagenomic analysis of two enhanced biological
26 phosphorus removal (EBPR) sludge communities. Nat Biotech. 2006, 24, 1263-
27 1269.
- 28 [9] Okunuki, S., Kawaharasaki, M., Tanaka, H., Kanagawa, T., Changes in phosphorus
29 removing performance and bacterial community structure in an enhanced biological
30 phosphorus removal reactor. Water Res. 2004, 38, 2432-2438.
- 31 [10] Keasling, J.D., Dien, S.J.V., Pramanik, J., Engineering polyphosphate metabolism
32 in *Escherichia coli*: Implications for bioremediation of inorganic contaminants.
33 Biotechnology and Bioengineering. 1998, 58, 231-239.
- 34 [11] Li, Q., Yu, Z., Shao, X., He, J., Li, L., Improved phosphate biosorption by bacterial
35 surface display of phosphate-binding protein utilizing ice nucleation protein. FEMS
36 Microbiol Lett. 2009, 299, 44-52.
- 37 [12] Hirota, R., Kuroda, A., Kato, J., Ohtake, H., Bacterial phosphate metabolism and its
38 application to phosphorus recovery and industrial bioprocesses. Journal of
39 Bioscience and Bioengineering. 2010, 109, 423-432.
- 40 [13] Choi, S.S., Lee, H.M., Ha, J.H., Kang, D.G., Kim, C.S., Seo, J.H., Cha, H.J.,
41 Biological Removal of Phosphate at Low Concentrations Using Recombinant
42 *Escherichia coli* Expressing Phosphate-Binding Protein in Periplasmic Space.

- 1 Applied biochemistry and biotechnology. 2013, 171, 1170-1177.
- 2 [14] Kato, J., Yamada, K., Muramatsu, A., Hardoyo, Ohtake, H., Genetic improvement
3 of *Escherichia coli* for enhanced biological removal of phosphate from wastewater.
4 Applied and Environmental Microbiology. 1993, 59, 3744-3749.
- 5 [15] Jones, K.L., Kim, S.-W., Keasling, J.D., Low-Copy Plasmids can Perform as Well
6 as or Better Than High-Copy Plasmids for Metabolic Engineering of Bacteria.
7 Metabolic Engineering. 2000, 2, 328-338.
- 8 [16] Akiyama, M., Croke, E., Kornberg, A., The polyphosphate kinase gene of
9 *Escherichia coli*. Isolation and sequence of the *ppk* gene and membrane location of
10 the protein. J Biol Chem. 1992, 267, 22556-22561.
- 11 [17] Rao, N.N., Gomez-Garcia, M.R., Kornberg, A., Inorganic Polyphosphate: Essential
12 for Growth and Survival. Annual Review of Biochemistry. 2009, 78, 605-647.
- 13 [18] Akiyama, M., Croke, E., Kornberg, A., An exopolyphosphatase of *Escherichia*
14 *coli*. The enzyme and its *ppx* gene in a polyphosphate operon. Journal of Biological
15 Chemistry. 1993, 268, 633-639.
- 16 [19] Alvarado, J., Ghosh, A., Janovitz, T., Jauregui, A., Hasson, M.S., Sanders, D.A.,
17 Origin of exopolyphosphatase processivity: Fusion of an ASKHA
18 phosphotransferase and a cyclic nucleotide phosphodiesterase homolog. Structure.
19 2006, 14, 1263-1272.
- 20 [20] Keasling, J.D., Bertsch, L., Kornberg, A., Guanosine pentaphosphate
21 phosphohydrolase of *Escherichia coli* is a long-chain exopolyphosphatase.
22 Proceedings of the National Academy of Sciences of the United States of America.
23 1993, 90, 7029-7033.
- 24 [21] Kuroda, A., Murphy, H., Cashel, M., Kornberg, A., Guanosine tetra- and
25 pentaphosphate promote accumulation of inorganic polyphosphate in *Escherichia*
26 *coli*. J Biol Chem. 1997, 272, 21240-3.
- 27 [22] Croke, E., Akiyama, M., Rao, N.N., Kornberg, A., Genetically altered levels of
28 inorganic polyphosphate in *Escherichia coli*. J Biol Chem. 1994, 269, 6290-6295.
- 29 [23] Grillo-Puertas, M., Villegas, J.M., Rintoul, M.R., Rapisarda, V.A., Polyphosphate
30 degradation in stationary phase triggers biofilm formation via LuxS quorum sensing
31 system in *Escherichia coli*. PLoS One. 2012, 7, e50368.
- 32 [24] Kerfeld, C.A., Sawaya, M.R., Tanaka, S., Nguyen, C.V., Phillips, M., Beeby, M.,
33 Yeates, T.O., Protein structures forming the shell of primitive bacterial organelles.
34 Science. 2005, 309, 936-938.
- 35 [25] Pang, A., Liang, M., Prentice, M.B., Pickersgill, R.W., Substrate channels revealed
36 in the trimeric *Lactobacillus reuteri* bacterial microcompartment shell protein PduB.
37 Acta crystallographica. Section D, Biological crystallography. 2012, 68, 1642-1652.
- 38 [26] Kerfeld, C.A., Heinhorst, S., Cannon, G.C., Bacterial Microcompartments. Annual
39 Review of Microbiology. 2010, 64, 391-408.
- 40 [27] Jorda, J., Lopez, D., Wheatley, N.M., Yeates, T.O., Using comparative genomics to
41 uncover new kinds of protein-based metabolic organelles in bacteria. Protein
42 Science. 2013, 22, 179-195.
- 43 [28] Niklowitz, W., Drews, G., Beiträge zur Cytologie der Blaualgen [Cytology of blue
44 algae. IV. Comparative electron microscopic studies on the substructure of some
45 Hormogonales]. Archives of Microbiology. 1956, 24, 134-146.
- 46 [29] Shively, J.M., Bradburne, C.E., Aldrich, H.C., Bobik, T.A., Mehlman, J.L., Jin, S.,

- 1 Baker, S.H., Sequence homologs of the carboxysomal polypeptide CsoS1 of the
2 thiobacilli are present in cyanobacteria and enteric bacteria that form carboxysomes
3 - polyhedral bodies. Canadian Journal of Botany-Revue Canadienne De Botanique.
4 1998, 76, 906-916.
- 5 [30] Axen, S.D., Erbilgin, O., Kerfeld, C.A., A taxonomy of bacterial microcompartment
6 loci constructed by a novel scoring method. PLoS Comput Biol. 2014, 10,
7 e1003898.
- 8 [31] Dou, Z., Heinhorst, S., Williams, E.B., Murin, C.D., Shively, J.M., Cannon, G.C.,
9 CO₂ Fixation Kinetics of Halothiobacillus neapolitanus Mutant Carboxysomes
10 Lacking Carbonic Anhydrase Suggest the Shell Acts as a Diffusional Barrier for
11 CO₂. J. Biol. Chem. 2008, 283, 10377-10384.
- 12 [32] Sampson, E.M., Bobik, T.A., Microcompartments for B12-dependent 1,2-
13 propanediol degradation provide protection from DNA and cellular damage by a
14 reactive metabolic intermediate. J Bacteriol. 2008, 190, 2966-2971.
- 15 [33] Penrod, J.T., Roth, J.R., Conserving a Volatile Metabolite: a Role for
16 Carboxysome-Like Organelles in Salmonella enterica. J. Bacteriol. 2006, 188,
17 2865-2874.
- 18 [34] Thiennimitr, P., Winter, S.E., Winter, M.G., Xavier, M.N., Tolstikov, V., Huseby,
19 D.L., Sterzenbach, T., Tsois, R.M., Roth, J.R., Bäumler, A.J., Intestinal
20 inflammation allows Salmonella to use ethanolamine to compete with the
21 microbiota. Proceedings of the National Academy of Sciences. 2011, 108, 17480-
22 17485.
- 23 [35] Bertin, Y., Girardeau, J.P., Chaucheyras-Durand, F., Lyan, B., Pujos-Guillot, E.,
24 Harel, J., Martin, C., Enterohaemorrhagic Escherichia coli gains a competitive
25 advantage by using ethanolamine as a nitrogen source in the bovine intestinal
26 content. Environmental Microbiology. 2011, 13, 365-377.
- 27 [36] Parsons, J.P., Dinesh, S.D., Deery, E., Leech, H.K., Brindley, A.A., Heldt, D.,
28 Frank, S., Smales, C.M., Lunsdorf, H., Rambach, A., Gass, M.H., Bleloch, A.,
29 McClean, K.J., Munro, A.W., Rigby, S.E.J., Warren, M.J., Prentice, M.B.,
30 Biochemical and structural insights into bacterial organelle form and biogenesis. J.
31 Biol. Chem. 2008, 283, 14366-14375.
- 32 [37] Parsons, J.B., Frank, S., Bhella, D., Liang, M., Prentice, M.B., Mulvihill, D.P.,
33 Warren, M.J., Synthesis of Empty Bacterial Microcompartments, Directed
34 Organelle Protein Incorporation, and Evidence of Filament-Associated Organelle
35 Movement. Molecular Cell. 2010, 38, 305-315.
- 36 [38] Fan, C., Cheng, S., Liu, Y., Escobar, C.M., Crowley, C.S., Jefferson, R.E., Yeates,
37 T.O., Bobik, T.A., Short N-terminal sequences package proteins into bacterial
38 microcompartments. Proc Natl Acad Sci U S A. 2010, 107, 7509-14.
- 39 [39] Lawrence, A.D., Frank, S., Newnham, S., Lee, M.J., Brown, I.R., Xue, W.-F.,
40 Rowe, M.L., Mulvihill, D.P., Prentice, M.B., Howard, M.J., Warren, M.J., Solution
41 structure of a bacterial microcompartment targeting peptide and its application in
42 the construction of an ethanol bioreactor. ACS Synthetic Biology. 2014, 3, 454-465.
- 43 [40] Martin, W., Koonin, E.V., Introns and the origin of nucleus-cytosol
44 compartmentalization. Nature. 2006, 440, 41-45.
- 45 [41] Choudhary, S., Quin, M.B., Sanders, M.A., Johnson, E.T., Schmidt-Dannert, C.,
46 Engineered Protein Nano-Compartments for Targeted Enzyme Localization. PLoS

- 1 ONE. 2012, 7, e33342.
- 2 [42] Schaffer, D.V., Koerber, J.T., Lim, K.-i., Molecular Engineering of Viral Gene
3 Delivery Vehicles. Annual Review of Biomedical Engineering. 2008, 10, 169-194.
- 4 [43] Worsdorfer, B., Woycechowsky, K.J., Hilvert, D., Directed evolution of a protein
5 container. Science. 2011, 331, 589-592.
- 6 [44] Neidhardt, F.C., Bloch, P.L., Smith, D.F., Culture Medium for Enterobacteria. J.
7 Bacteriol. 1974, 119, 736-747.
- 8 [45] Sambrook, J., Russell, D.W. 2001. Molecular Cloning: A Laboratory Manual,
9 (eds.), Cold Spring Harbor Laboratory Press, Woodbury NY.
- 10 [46] Sinha, S., Cheng, S., Fan, C., Bobik, T.A., The PduM protein is a structural
11 component of the microcompartments involved in coenzyme B12-dependent 1,2-
12 propanediol degradation by Salmonella. Journal of Bacteriology. 2012, 194, 1912-
13 1918.
- 14 [47] Sriramulu, D.D., Liang, M., Hernandez-Romero, D., Raux-Deery, E., Lunsdorf, H.,
15 Parsons, J.B., Warren, M.J., Prentice, M.B., Lactobacillus reuteri DSM 20016
16 produces cobalamin-dependent diol dehydratase in metabolosomes and metabolises
17 1,2-propanediol by disproportionation. J Bacteriol. 2008, 190, 4559-4567.
- 18 [48] Nahálka, J., Gemeiner, P., Bučko, M., Wang, P.G., Bioenergy Beads: A Tool for
19 Regeneration of ATP/NTP in Biocatalytic Synthesis. Artificial Cells, Blood
20 Substitutes and Biotechnology. 2006, 34, 515-521.
- 21 [49] Amado, L., Kuzminov, A., Polyphosphate Accumulation in Escherichia coli in
22 Response to Defects in DNA Metabolism. J. Bacteriol. 2009, 191, 7410-7416.
- 23 [50] Ault-Riche, D., Fraley, C.D., Tzeng, C.-M., Kornberg, A., Novel Assay Reveals
24 Multiple Pathways Regulating Stress-Induced Accumulations of Inorganic
25 Polyphosphate in Escherichia coli. J. Bacteriol. 1998, 180, 1841-1847.
- 26 [51] Mullan, A., Quinn, J.P., McGrath, J.W., A nonradioactive method for the assay of
27 polyphosphate kinase activity and its application in the study of polyphosphate
28 metabolism in Burkholderia cepacia. Analytical Biochemistry. 2002, 308, 294-299.
- 29 [52] Kulakova, A.N., Hobbs, D., Smithen, M., Pavlov, E., Gilbert, J.A., Quinn, J.P.,
30 McGrath, J.W., Direct Quantification of Inorganic Polyphosphate in Microbial
31 Cells Using 4'-6-Diamidino-2-Phenylindole (DAPI). Environmental Science &
32 Technology. 2011, 45, 7799-7803.
- 33 [53] Bradford, M.M., A rapid and sensitive method for the quantitation of microgram
34 quantities of protein utilizing the principle of protein-dye binding. Analytical
35 biochemistry. 1976, 72, 248-254.
- 36 [54] Standard Methods for the Examination of Water and Wastewater. 2005, American
37 Public Health Association; 2005
- 38 [55] Serafim, L.S., Lemos, P.C., Levantesi, C., Tandoi, V., Santos, H., Reis, M.A.M.,
39 Methods for detection and visualization of intracellular polymers stored by
40 polyphosphate-accumulating microorganisms. Journal of Microbiological Methods.
41 2002, 51, 1-18.
- 42 [56] Spurr, A.R., A Low-Viscosity Epoxy Resin Embedding Medium for Electron
43 Microscopy. Journal of Ultrastructure Research. 1969, 26, 31-43.
- 44 [57] Lünsdorf, H., Strömpl, C., Osborn, A.M., Bennisar, A., Moore, E.R., Abraham,
45 W.R., Timmis, K.N., Approach to analyze interactions of microorganisms,
46 hydrophobic substrates, and soil colloids leading to formation of composite

- 1 biofilms, and to study initial events in microbiogeological processes. *Methods*
2 *Enzymol.* 2001, 336, 317-331.
- 3 [58] Bond, P.L., Keller, J., Blackall, L.L., Anaerobic phosphate release from activated
4 sludge with enhanced biological phosphorus removal. A possible mechanism of
5 intracellular pH control. *Biotechnology and Bioengineering.* 1999, 63, 507-515.
- 6 [59] Ahn, K., Kornberg, A., Polyphosphate kinase from *Escherichia coli*. Purification
7 and demonstration of a phosphoenzyme intermediate. *J Biol Chem.* 1990, 265,
8 11734-11739.
- 9 [60] Whitehead, M.P., Eagles, L., Hooley, P., Brown, M.R.W., Most bacteria synthesize
10 polyphosphate by unknown mechanisms. *Microbiology.* 2014, 160, 829-831.
- 11 [61] Sharfstein, S.T., Keasling, J.D., Polyphosphate Metabolism in *Escherichia coli*.
12 *Annals of the New York Academy of Sciences.* 1994, 745, 77-91.
- 13 [62] Kato, J., Yamamoto, T., Yamada, K., Ohtake, H., Cloning, sequence and
14 characterization of the polyphosphate kinase-encoding gene (ppk) of *Klebsiella*
15 *aerogenes*. *Gene.* 1993, 137, 237-242.
- 16 [63] Morohoshi, T., Maruo, T., Shirai, Y., Kato, J., Ikeda, T., Takiguchi, N., Ohtake, H.,
17 Kuroda, A., Accumulation of inorganic polyphosphate in *phoU* mutants of
18 *Escherichia coli* and *Synechocystis sp. strain PCC6803*. *Appl Environ Microbiol.*
19 2002, 68, 4107-4110.
- 20 [64] Rao, N.N., Roberts, M.F., Torriani, A., Amount and chain length of polyphosphates
21 in *Escherichia coli* depend on cell growth conditions. *J. Bacteriol.* 1985, 162, 242-
22 247.
- 23 [65] Van Dien, S.J., Keyhani, S., Yang, C., Keasling, J.D., Manipulation of independent
24 synthesis and degradation of polyphosphate in *Escherichia coli* for investigation of
25 phosphate secretion from the cell. *Applied and Environmental Microbiology.* 1997,
26 63, 1689-1695.
- 27 [66] Zhang, X., Konarev, P.V., Petoukhov, M.V., Svergun, D.I., Xing, L., Cheng, R.H.,
28 Haase, I., Fischer, M., Bacher, A., Ladenstein, R., Meining, W., Multiple Assembly
29 States of Lumazine Synthase: A Model Relating Catalytic Function and Molecular
30 Assembly. *Journal of Molecular Biology.* 2006, 362, 753-770.
- 31 [67] Seebeck, F.P., Woycechowsky, K.J., Zhuang, W., Rabe, J.P., Hilvert, D., A Simple
32 Tagging System for Protein Encapsulation. *Journal of the American Chemical*
33 *Society.* 2006, 128, 4516-4517.
- 34 [68] Laplagne, D.A., Zylberman, V., Ainciart, N., Steward, M.W., Sciutto, E., Fossati,
35 C.A., Goldbaum, F.A., Engineering of a polymeric bacterial protein as a scaffold
36 for the multiple display of peptides. *Proteins: Structure, Function, and*
37 *Bioinformatics.* 2004, 57, 820-828.
- 38 [69] Wu, W., Xing, L., Zhou, B., Lin, Z., Active protein aggregates induced by
39 terminally attached self-assembling peptide ELK16 in *Escherichia coli*. *Microbial*
40 *Cell Factories.* 2011, 10, 9.
- 41 [70] Nahalka, J., Patoprsty, V., Enzymatic synthesis of sialylation substrates powered by
42 a novel polyphosphate kinase (PPK3). *Organic & Biomolecular Chemistry.* 2009, 7,
43 1778-1780.
- 44 [71] Herr, A., Fischer, R., Improvement of *Aspergillus nidulans* penicillin production by
45 targeting *AcvA* to peroxisomes. *Metab Eng.* 2014, 25, 131-139.
- 46 [72] Johnson, C.L., Pechonick, E., Park, S.D., Havemann, G.D., Leal, N.A., Bobik, T.A.,

- 1 Functional genomic, biochemical, and genetic characterization of the Salmonella
2 pduO gene, an ATP:cob(I)alamin adenosyltransferase gene. J Bacteriol. 2001, 183,
3 1577-84.
- 4 [73] Achbergerová, L., Nahálka, J., Polyphosphate - an ancient energy source and active
5 metabolic regulator. Microbial Cell Factories. 2011, 10, 63.
- 6 [74] Kuroda, A., Takiguchi, N., Gotanda, T., Nomura, K., Kato, J., Ikeda, T., Ohtake,
7 H., A simple method to release polyphosphate from activated sludge for phosphorus
8 reuse and recycling. Biotechnology and Bioengineering. 2002, 78, 333-338.
- 9

10

11

12 **Acknowledgements**

13 This research was supported by Health Research Board award HRA_POR/2011/111 to
14 MBP, and has emanated from research supported in part by Science Foundation Ireland
15 (SFI) under Grant Numbers 11/TIDA/B2001 and SFI/12/RC/2273. It was also supported
16 by grants from the British Biotechnology and Biological Sciences Research Council
17 (BBSRC), BB/M002969 and BB/H013180. MBP, MJW, ML are named co-inventors on
18 US Patent US9187766 (B2) (also currently WO2013045562 (A1), EP2760883 (A1))
19 “Accumulation of metabolic products in bacterial microcompartments”.

20

21

Table 1
Plasmids and strains used in this study

Plasmids and strains	Genotype*	Source
Plasmids		
pET23b	pBR322, T7 Ap	Novagen
pCOLADuet-1™	ColA ori lacI T7lac Kan ^r	Novagen
pLysS	p15A Cam ^R	Novagen
pET23b- PduP18-GFP	pET23b with <i>pduP18</i> [†] leader sequence and <i>gfp</i> [▲]	Prof. Martin Warren, University of Kent
pLysS-PduABJKNU (pSF37)	Cam ^R , Tet ^R <i>pduABJKNU</i> [†]	[37]
pML001	pET23b with <i>pduP18</i> [†] - <i>ppk1</i> fusion without <i>gfp</i> [▲]	This study
pML002	pET23b- <i>ppk1</i>	This study
pCOLADuetPPK (pYY002)	pCOLADuet-1 with <i>ppk1</i>	This study
pCOLADuetP18PPK (pYY010)	pCOLADuet-1 with <i>pduP18</i> [†] - <i>ppk1</i> fusion	This study
pCOLADuetPPXPPK (pYY005)	pCOLADuet-1 with <i>ppk1</i> and <i>ppx</i>	This study
pCOLADuetP18PPKPPX (pYY007)	pCOLADuet-1 with <i>pduP18</i> [†] - <i>ppk1</i> fusion and <i>ppx</i>	This study
pCOLADuetD60PPXP18PPK (pYY008)	pCOLADuet-1 with <i>ppk1</i> and <i>pduD60</i> [†] - <i>ppx</i> fusion	This study
Strains		
<i>E. coli</i> JM109	<i>endA1 glnV44 thi-1 relA1 gyrA96 recA1 mcrB</i> ⁺ Δ (<i>lac-proAB</i>) <i>e14- hsdR17</i> (<i>rK</i> ⁺ <i>mK</i> ⁺)	Promega
<i>E. coli</i> Top 10	<i>F- mcrA</i> Δ (<i>mrr-hsdRMS-mcrBC</i>) ϕ 80 <i>lacZAM15</i> Δ <i>lacX74 nupG recA1 araD139</i> Δ (<i>ara-leu</i>)7697 <i>galE15 galK16 rpsL</i> (<i>Str</i> ^R) <i>endA1</i> λ ⁻	Invitrogen
<i>E. coli</i> BL21 (DE3)	<i>F</i> ⁻ <i>ompT hsdS_B</i> (<i>r_B</i> <i>m_B</i>) <i>gal dcm</i> (DE3)	Stratagene
<i>E. coli</i> Tuner (DE3)	<i>F</i> ⁻ <i>ompT hsdS_B</i> (<i>r_B</i> <i>m_B</i>) <i>gal dcm lacY1</i> (DE3)	Stratagene

*All inserts from *E. coli* JM109 unless specified [†]From *Citrobacter freundii* [▲]From *Aequorea victoria*

Figures

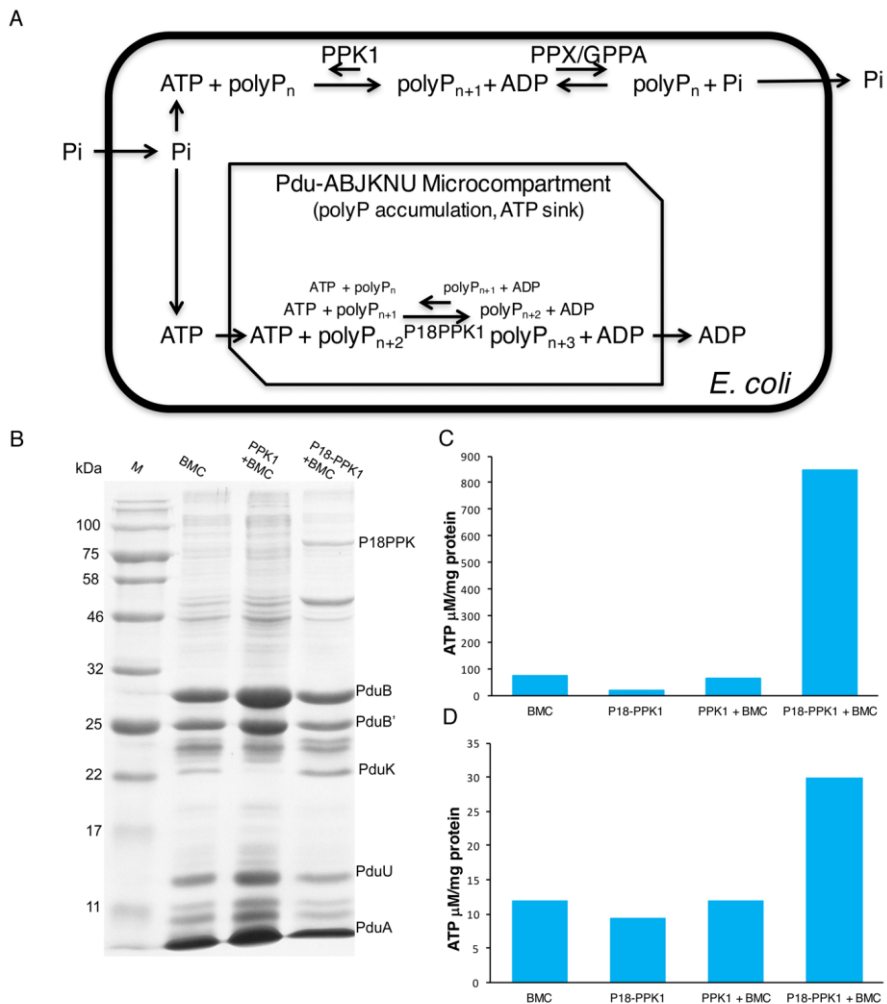


Fig. 1. The effect of microcompartment-targeting of polyphosphate kinase (PPK1) on polyphosphate metabolism in *E. coli*

A. Proposed mechanism of increasing polyphosphate content of *E. coli* by microcompartment-targeting of polyphosphate kinase (PPK1). B. SDS-PAGE gel of microcompartment samples isolated from various *E. coli* BL21 (DE3) strains. M: MW marker. BMC: empty microcompartments only, (pSF37). PPK1 + BMC : non-targeted PPK1 plus microcompartments (pML002 + pSF37). P18-PPK1+ BMC: microcompartment-targeted P18-PPK1 plus microcompartments (pML001+ pSF37). C. Polyphosphate kinase assay on isolated microcompartments with addition of ADP and polyphosphate. D. Polyphosphate kinase assay on isolated microcompartments with addition of ADP alone. In C and D the

second column represents a control microcompartment extraction procedure from **pLysS containing** cells expressing P18-PPK alone without microcompartments.

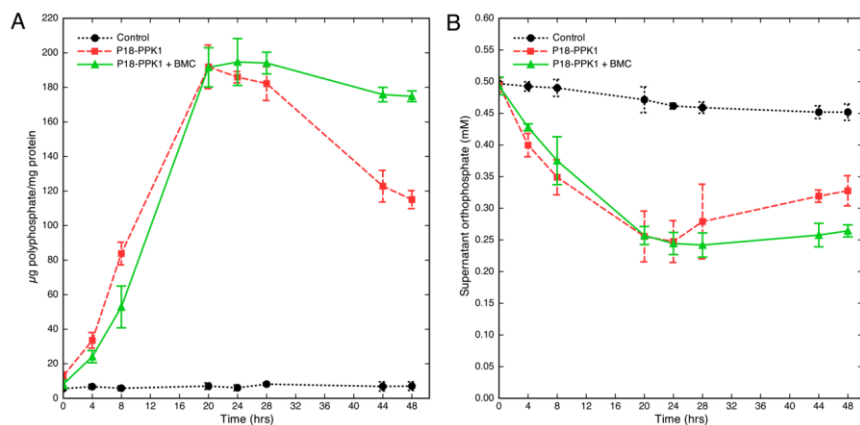


Fig. 2. Co-expression of targeted PPK1 and recombinant microcompartments in *E. coli* results in stable orthophosphate uptake and polyphosphate retention.

A. Polyphosphate content of whole cells over 48 hours. B. Orthophosphate concentration in culture medium over 48 hours. Dashed line with filled circles: *E. coli* BL21 (DE3) pLysS control. Continuous red line with filled squares : P18-PPK1, microcompartment-targeted PPK1 (pML001 + pLysS). Continuous green line with filled triangles : P18-PPK1 + BMC, microcompartment-targeted P18-PPK1 plus microcompartments (pML001 + pSF37). Error bars represent standard deviation of three independent observations.

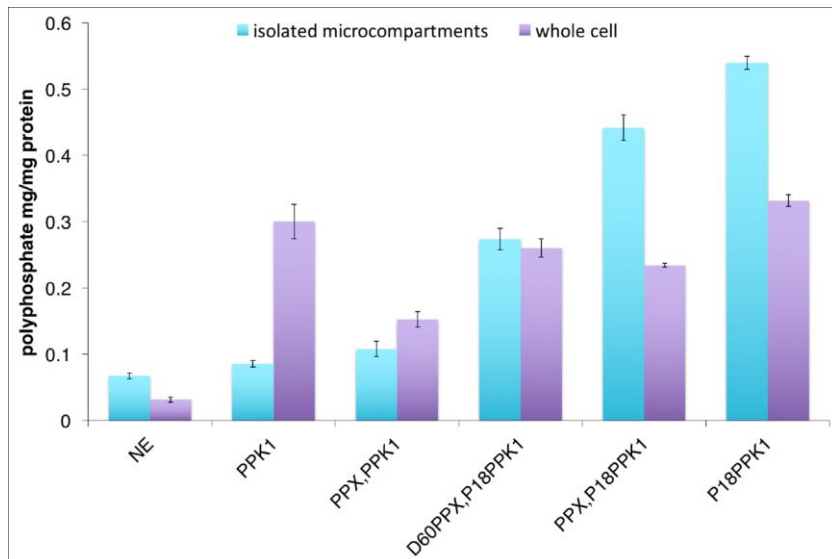


Fig. 3. Co-expression of microcompartment-targeted PPK1 and recombinant microcompartments in *E. coli* increases the polyphosphate content of isolated microcompartments and protects polyphosphate from co-expressed cytoplasmic polyphosphatase.

Polyphosphate content of isolated microcompartments (blue bars) and whole cells (purple bars) measured with a DAPI assay following overnight culture. All *E. coli* BL21 (DE3) strains were expressing microcompartments (pSF37) and in addition various combinations of targeted and un-targeted PPK1 and PPX. BMC: microcompartments only, (pSF37). PPK1 + BMC: non-targeted PPK1 and microcompartments, (pML002 + pSF37). PPK1 + PPX + BMC: non-targeted PPK1 and non-targeted PPX and microcompartments (pYY005 + pSF37). P18-PPK1 + D60PPX + BMC : targeted PPK1 and targeted PPX and microcompartments (pYY08+ pSF37) . P18-PPK1 + PPX + BMC: targeted PPK1 and non-targeted PPX and microcompartments (pYY07 + pSF37). P18-PPK1 + BMC: targeted PPK1 and microcompartments (pYY010 + pSF37). Error bars represent standard deviation of three independent observations.

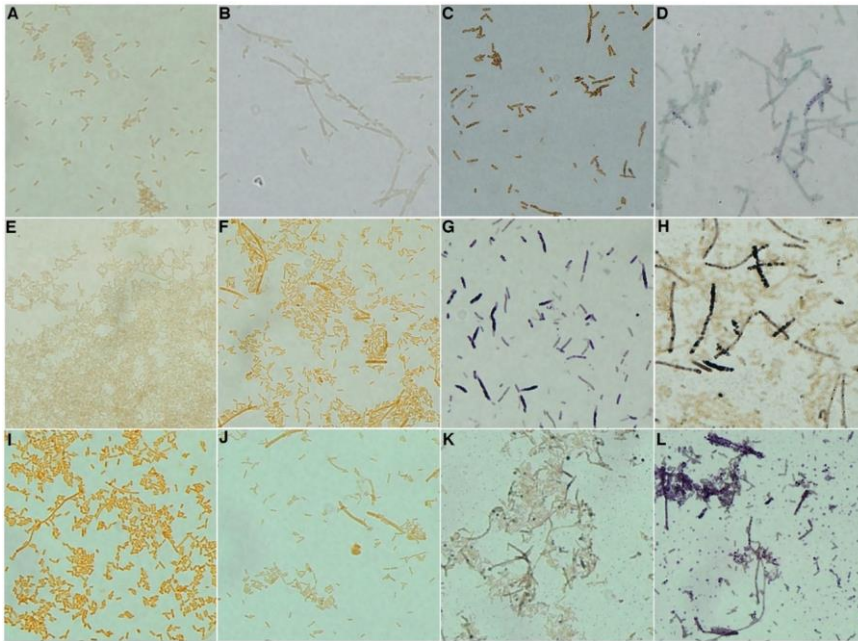


Fig. 4. Co-expression of targeted PPK1 and recombinant microcompartments in *E. coli* results in cytoplasmic polyphosphate granule formation persisting into stationary phase. Light microscopy of Neisser stained fixed cells (toluidine blue and chrysoidine counterstain, polyphosphate appears purple-black, predominantly yellow cells are polyphosphate-free). A,E,I: control *E. coli* BL21 (DE3) pLysS. B,F,J: *E. coli* BL21 (DE3) BMC, microcompartments only (pSF37). C,G,K: *E. coli* BL21 (DE3) P18-PPK1, targeted PPK1 (pML001 + pLysS). D,H,L: *E. coli* BL21 (DE3) P18-PPK1 + BMC, targeted PPK1 plus microcompartments (pML001 + pSF37). Incubation time in MOPS : A,B,C,D 4 hours, E,F,G,H 18 hours, I,J,K,L 44 hours.

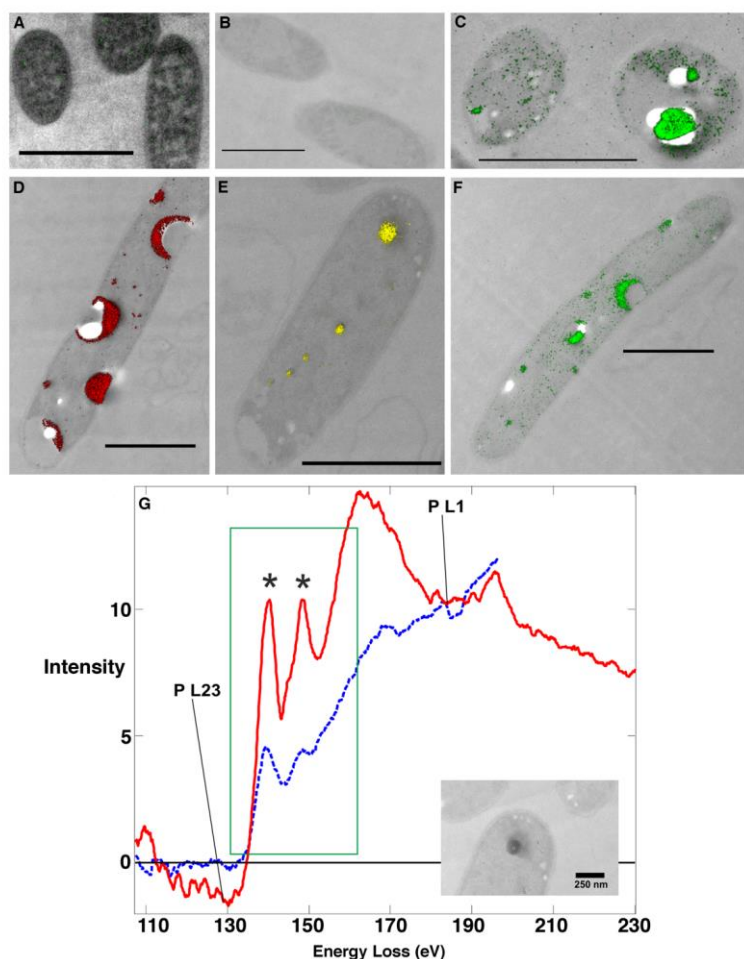


Fig. 5. Phosphorus content of cytoplasmic granules in *E. coli* expressing recombinant polyphosphate kinase is confirmed by ultrastructural and electron-loss spectroscopic analysis using energy-filtered transmission electron microscopy (EFTEM) and is increased and qualitatively altered by recombinant microcompartment co-expression
 A: control *E. coli* TunerTM(DE3). B: *E. coli* TunerTM (DE3) BMC, microcompartment only (pSF37). C: *E. coli* BL21 (DE3) P18-PPK1, targeted PPK1 (pML001+ pLysS). D,E,F,G: *E. coli* TunerTM (DE3) P18-PPK1 + BMC, targeted PPK1 plus microcompartments (pML001 + pSF37). A-F: Electron spectroscopic imaging. Phosphorus signals are shown as overlays: green in A,B,C,F; red in D; yellow in E. Scale bar 1 μ m unless stated. G: Parallel electron

energy-loss spectroscopy (PEELS) of the largest granule in E. The red line represents SpotPEELS of the large inclusion from E with the spot (size: 16 nm) placed centrally (electron micrograph inset). The green-boxed area represents the P-L_{2,3} energy-loss near-edge structure (ELNES), characterized by the two peaks (asterisks). The blue-coloured dashed spectrum is referenced from sodium polyphosphate.